Scalability of the Environmental Impacts of Pit Thermal Energy Storage: An Approach to Extrapolate the Global Warming Potential

Richard Lüchinger[1], Pauline Fuchs [2], Philipp Schuetz[1], Jörg Worlitschek[1], Heimo Walter[2]

[1] Competence Centre Thermal Energy Storage, Lucerne University of Applied Sciences and Arts, Lucerne, Switzerland

[2] Institute for Energy Systems and Thermodynamics, TU Wien, Vienna, Austria

Abstract

Pit Thermal Energy Storage (PTES) can enable seasonal load shifting, but reliable environmental indicators are lacking in early planning phases. The goal is to provide a reliable estimate of the global warming potential (GWP) without a complete life cycle assessment (LCA) for each variant. Our contribution comprises four elements: We create a transparent life cycle inventory and life cycle impact assessment (LCIA) for a referenced PTES, identify the GWP driver, derive simple geometric scalings, and provide directly usable GWP values over volume. Methodologically, we combine a prospective LCA with a geometry-based scaling of the impact driver. Two cover variants are balanced and prove to be practically equivalent. The LCIA results in a total of ≈ 5.24×105 kg CO2-eq, specifically ≈ 76 kg CO2-eq/MWh and ≈ 6.9 kg CO2-eq/m³. The drivers are the covering materials, PE foam and high-density polyethylene (HDPE), together accounting for ≈ 61%. For scaling, we use an additive multi-term model: area proportions ∝ $V^{2/3}$, volume proportions ∝ V, with a small remainder remaining constant. Specific emissions decrease sublinearly, with a power fit yielding b ≈ −0.28. This results in clear priorities for planning: optimize coverage and select size specifically.

Keywords: pit thermal energy storage, seasonal thermal energy storage, life cycle assessment, impact driver, scaling analysis, early-stage environmental assessment

Nomenclature

Quantity / Term	Symbol	Unit
Area	A	m²
Aquifer thermal energy storage	ATES	
Borehole thermal energy storage	BTES	
Constant residual	C	kg CO_2-eq
Cover proportionality	k_{lid}	m² / $m^{2/3}$
Geometric variable	$X_i(V)$	unit of X
Global Warming Potential	GWP	kg CO_2-eq
Global Warming Potential, 100 y	GWP100	kg CO_2-eq
High-density polyethylene	HDPE	
Intensity of term i	α_i	kg CO_2-eq per unit
Layer thickness	t	m
Length	L	m
Lid area	A_{lid}	m²
Life cycle assessment	LCA	
Life Cycle Impact Assessment	LCIA	
Life Cycle Inventory	LCI	
Material density	ρ	kg/m³
Pit thermal energy storage	PTES	
Power-law coefficient	a	kg CO_2-eq/MWh
Power-law exponent	b	
Proportionality constant	k_i	unit
ReCiPe 2016 Midpoint (H)	ReCiPe-H	
Reference volume	V0	m³
Scaling exponent	p_i	
Seasonal thermal energy storage	STES	
Specific GWP (energy)	$GWP_{spec}(V)$	kg CO_2-eq/MWh
Storage height	H	m
Tank thermal energy storage	TTES	
Total GWP at size V	$GWP_{tot}(V)$	kg CO_2-eq
Volume	V	m³

10.18086/swc.2025.09.18 Available at http://proceedings.ises.org

1. Introduction

STES offers a promising approach to storing large amounts of thermal energy over a period of months, thus decoupling supply and demand over seasons(Xu et al., 2014). This storage possibility facilitates the exploitation of the previously untapped potential of renewable energy sources, in particular solar energy (Shah et al., 2018; Zhang et al., 2015) and reduces the dependence on fossil fuels (de Gracia & Cabeza, 2015; Yang et al., 2021). Among the available concepts, we are considering Pit Thermal Energy Storage (PTES). PTES has been tested on an industrial scale, offers a favorable volume-to-area ratio, and has low specific costs in the temperature range of approximately 10 to 95 °C (Lüchinger et al., 2025; Sifnaios, 2023).

However, to the best of the authors' knowledge, there is a lack of reliable environmental indicators for PTES in scientific literature. These are particularly crucial in the early planning stages, as this is when the course is set. Comprehensive life cycle assessments (LCA) provide well-founded results, but they require time and detailed data that is rarely available at the start of a project. What is needed are LCAs and statements about the ecological footprint of PTES, as well as insights into how global warming potential (GWP) changes with plant size.

The aim of this study is to develop tools for estimating the GWP of PTES in early stages without performing a complete LCA for each variable. To this end, we combine a prospective LCA with a scaling evaluation of the dominant contribution source. From the life cycle impact assessment (LCIA) of the reference system, we identify the impact driver and derive simple, geometry-based scaling functions. Our contribution consists of four parts: First, we create a transparent Life Cycle Inventory (LCI) and LCIA for the referenced PTES. Second, we identify the GWP impact driver of PTES. Third, we show that the impact is easily scalable using a few geometric terms and that specific emissions decrease sublinearly with increasing volume. Fourth, we provide manageable GWP values as a function of volume, including uncertainty bands, which can be used directly in planning.

The paper is structured as follows: Section 2 outlines the state of research on STES and describes the reference system. Section 3 explains the methodology, system boundaries, and functional unit and justifies key assumptions. Section 4 presents the LCI and LCIA results, quantifies the scaling of the GWP, discusses the main limitations, and provides an outlook on future work. Section 5 concludes the paper.

2. State of Research on PTES and Environmental Assessment

STES systems store heat for weeks or months, thereby balancing seasonal fluctuations between energy supply and demand (Bott et al., 2019; Xu et al., 2014). Depending on the physical principle, three basic types of storage are distinguished (Alva et al., 2018): sensible storage, latent storage, and thermochemical storage. Due to their higher technical maturity (see Sträter et al., (2025)), this study focuses on sensible heat storage. These use the temperature change of a medium, usually water or soil, to store and release heat (Alva et al., 2018). The following sections provide an overview of the PTES technology and the state of ecological research on STES.

2.1. Pit Thermal Energy Storage (PTES)

PTES is a promising and cost-effective technology for large-scale heat storage (Sifnaios, 2023; Xiang et al., 2022). The system consists of an earthen basin filled with water, lined with a waterproof membrane and protected against heat loss by a floating, insulated cover (Sorknæs, 2018). In some projects, gravel is added to the water, however, this aspect is not further considered here. PTES is characterized by low heat loss, high energy density, and low specific costs at operating temperatures of approximately 10 to 95 °C. Due to the favorable volume-to-surface ratio, these storage systems are particularly suitable for large facilities in rural or suburban areas (Xiang et al., 2022; Yang et al., 2021). Despite the technical advantages, their use has remained limited: between 1987 and 2023, only 13 PTES systems were documented (Sifnaios, 2023).

This paper uses the PTES SUNSTORE 4 system in Marstal, Denmark as a reference system because it is well documented by Jensen & PlanEnergi, (2014), Sifnaios et al., (2022) and Sørensen & Schmidt, (2018). Built between 2011/2012, the storage facility has a total volume of around 76 000 m³ and a storage capacity of 6.96 GWh. It operates within a temperature range of 10 to 90 °C and is integrated into the local district heating network. It consists of a pit with a 1:2 slope gradient, sealed at the bottom and sides by a 2 mm-thick HDPE geomembrane, which is in turn lined with a geotextile. The cover is a floating structure consisting of three layers of dimpled foam sandwiched between an upper and lower geomembrane. A Hypernet fabric is located between the layers to ventilate and separate them. A system of HDPE weight pipes filled with concrete was originally used to stabilize and shape the cover. These pipes created a slight slope towards the center to direct rainwater to the central pump sump. In practice, however, this solution was costly and only partially effective. Consequently, in 2019/2020, the cover was replaced with a segmented construction incorporating a gravel layer that performs the same function. Three stainless steel pipes enable layered loading and unloading at different temperature levels.

2.2. Environmental Assessment of STES

To the best of the authors' knowledge, the ecological assessment of seasonal heat storage systems has not yet been extensively researched. There are only a few studies that systematically examine environmental aspects. These are often only dealt with marginally in the context of larger energy or economic analyses (Hayatina et al., 2023). The existing studies are predominantly based on LCA or simplified CO_2 balances. Welsch et al., (2018) combined ecological and economic considerations for a district heating system with borehole thermal energy storage (BTES). They showed that BTES can reduce greenhouse gas emissions, but that the benefits depend heavily on the subsidy conditions. Other case studies, such as those by Godinaud et al., (2024) for an aquifer thermal energy storage (ATES) system in Bordeaux or by Wu et al., 2024 for a BTES system in Canada, cite the operational phase and construction as the main sources of environmental impacts. Ni et al., (2020) and Pallotta et al., (2025) investigated coupled or alternative storage systems. Venettacci et al., (2022) showed that PCM storage systems have lower environmental impacts but higher costs.

The relevant literature predominantly adopts a cradle-to-gate perspective in terms of methodology. This covers raw material extraction, material production, transport, and on-site construction. The operational phase is usually left out, as its impact depends heavily on the connected energy system and the emissions generated during operation are primarily attributed to heat generation rather than storage (see, for example, Wu et al., 2024). The end-of-life phase is often neglected because its contribution to the GWP is low and there are methodological uncertainties, as reported in several studies (including Gaegauf et al., (2016) and Welsch et al., 2016). This study follows this established framework.

Despite this work, robust LCAs for PTES are to the best of our knowledge lacking. The focus so far has been on underground systems such as ATES and BTES. Nor has there been any investigation of how environmental impacts change with system size. This lack of scalability represents a key research gap, especially in early planning phases when decisions must be made even though complete LCAs are not yet available.

3. Methodological Approach

The method is based on the concept of prospective LCA according to Arvidsson et al. (2018) and expands on this with a scaling analysis of the dominant impact driver. The process is outlined in Figure 1. Based on the target definition and system boundaries, a technically plausible PTES model is constructed and calibrated using the SUNSTORE 4 reference system. The relevant material and energy flows are then collected and recorded as a life cycle inventory in openLCA 1.12.0 with ecoinvent 3.9.1 (system model cut-off). The impact assessment is performed using ReCiPe 2016 v1.03 Midpoint (H) and focuses on the GWP within a cradle-to-gate system boundary. The functional unit (FU) is kg CO_2-eq per MWh of annual stored heat at one cycle per year; in addition, values per m^3 of storage volume are reported. Based on the LCIA, the component contributions are determined and the largest contributor is identified as the impact driver. If its share is around 70 to 80 percent, we use a single-term approach with a small residual term. Otherwise, we use an additive multi-term approach with a small residual term (see section 3.1). We then systematically vary the geometry of the impact driver—for example, the surface areas or layer thicknesses—recalculate the GWP for each variant, and derive simple, size-dependent estimation functions from the resulting point sets. This approach provides a transparent LCI and LCIA for the reference PTES as well as scaling functions derived from it for early planning phases.

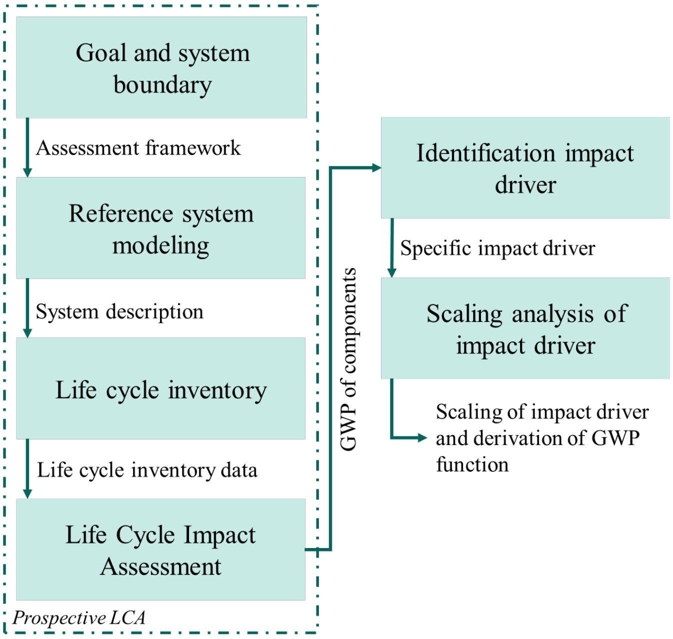

Figure 1: Methodical procedure of the prospective LCA (left) with subsequent scaling analysis of the respective impact driver (right).

3.1. Scaling Method

The goal is to develop a method for scaling the GWP_{100} of a PTES across different system sizes without having to recreate a complete life cycle assessment for each size. On this basis, GWP behavior can be estimated.

The basis is the LCIA of the reference system, from which the relative contribution shares of the components are determined; the proportionally largest GWP_{100} component is considered the impact driver. The functional logic and geometric relationships remain unchanged for all size variants. The contribution shares determine the choice of scaling approach; we define two different cases.

Case (1): There is a clearly dominant driver (≥ 70–80% of the total GWP). Scaling is performed using a single-term approach that describes the effect as the product of an intensity and a single geometric reference variable. A small constant surcharge can capture the remaining contributions in the size range under consideration. For the one-term approach, we couple a single geometric reference value with an impact-related intensity and add a constant surcharge (see Eq. 1).

$$GWP_{tot}(V) = \alpha_i \cdot X(V) + C \qquad \text{(Eq. 1)}$$

where: $GWP_{tot}(V)$: total GWP_{100} at size V [kg CO2-eq]; V: storage volume [m^3]; X(V): geometric reference variable (area/length/volume) [unit of X]; α_i: intensity per unit of X [kg CO2-eq per unit of X]; C: constant surcharge for residuals [kg CO2-eq].

Assuming the shape remains unchanged (with a constant slope angle and aspect ratio), the surface area will scale sublinearly with the volume. In the one-term model, we link the total GWP to the surface area via an area-related intensity and a small, fixed surcharge (see Eq. (2)). If the shape remains unchanged, the cover area can be estimated directly from the volume, and the proportionality constant can be derived from the reference case (see Eq. (3)). Substituting Eq. (3) into Eq. (2) yields the compact volume dependence of the total GWP, see Eq. (4).

$$GWP_{tot}(V) \approx \alpha_i \cdot A_{lid}(V) + C \quad \text{(Eq. 2)}$$

$$A_{lid}(V) \approx k_{lid} \cdot V^{\frac{2}{3}}, \quad with\ k_{lid} = \left(\frac{A_{lid}(V_0)}{V_0^{\frac{2}{3}}}\right) \quad \text{(Eq. 3)}$$

$$GWP_{tot}(V) \approx \alpha_i \cdot k_{lid} \cdot V^{\frac{2}{3}} + C \quad \text{(Eq. 4)}$$

where: $A_{lid}(V)$: lid area as a function of V [m^2] V_0 reference volume [m^3]; k_{lid}: proportionality constant from the reference case.

Since no single component in the reference case reaches the threshold value of ≥ 70–80%, we scale using an additive multi-term model according to Case 2.

Case (2): There is no sufficiently dominant single factor. Scaling is performed additively using multiple terms. Each term links an effect-related intensity to a precisely defined geometric variable. A small constant surcharge represents residual contributions that are not scaled geometrically, see Eq. (5).

$$GWP_{tot}(V) = \sum_{i=1}^{m} (\alpha_i \cdot X_i(V)) + C \quad \text{(Eq. 5)}$$

where: m the number of terms [–] is.

Under shape invariance (constant slope angle and constant aspect ratio), the geometric quantities can be approximated as powers of the volume; areas typically scale with $V^{2/3}$, lengths with $V^{1/3}$, and volumes with V, see Eq. (6) to (7).

$$X_i \approx K_i \cdot V^{p_i}, \quad with \quad K_i \approx \frac{X_i(V_0)}{V_0^{p_i}} \quad \text{(Eq. 6)}$$

$$GWP_{tot}(V) = \sum_{i=1}^{m} \alpha_i k_i V^{p_i} + C \quad \text{(Eq. 7)}$$

where: p_i: Scaling exponent [–]; k_i: Proportionality constant from the reference case.

The scaling is implemented mathematically using a Python model that maps the Case 2 approach. The input geometry comes from the reference case and serves as the starting point for a volume sweep under shape invariance. The scaling variables for cover and liner are calculated from the geometry. The model then provides GWP(V) and GWP_{spec}(V) and fits a power function. An uncertainty band is created via a ±20 percent variation of α_i.

3.2. Reference System Description

The reference system is based on PTES SUNSTORE 4 in Marstal (Denmark). A description of the system can be found in Chapter 2. The central components of the storage facility were modeled: the earthworks and geometry, the HDPE liner with geotextile underlay, the floating cover with PE foam insulation, and the stainless steel inlet/outlet system. Two cover variants were considered: (A) the original design with concrete-filled HDPE weight pipes and (B) the later introduced, updated variant with gravel ballast. Smaller components such as vacuum valves, manholes, welds, and anchor trenches were neglected due to their minor influence on the result.

The FU describes the stored thermal energy in MWh per year of a PTES with a specific storage volume and material configuration. For the calculation, it is assumed that the storage facility undergoes one charging cycle per year (higher values are technically possible) and with a storage capacity of 6.96 GWh.

The system boundary includes only the PTES itself, which consists of an earth basin storage tank with water content, a liner system, a cover, insulation, an inlet/outlet system, and a pump sump. The solar collector field, heating system, and distribution are not included. The analysis follows a cradle-to-gate approach and thus covers all processes up to the construction of the storage facility on site. The operating phase is not considered, as its influence depends heavily on the higher-level energy system into which the storage facility is integrated. Due to its low contribution and difficulty in quantification, the end-of-life phase is neglected.

4. Results and Discussion

4.1. Life Cycle Inventory (LCI)

This chapter presents the LCI of the modeled reference system. The goal is to transparently present the essential material and energy flows of the PTES, thus laying the groundwork for the subsequent LCIA.

The material quantities were derived from the reference storage system. To do so, we calculated the relevant areas, volumes, and masses based on the documented system geometry (see Table 2 in the Appendix). The system boundary and methodological assumptions follow the description given in Section 3.1. The density values, layer thicknesses, and material structures were obtained from the technical descriptions of the SUNSTORE-4 storage system and technical average values. All calculation steps and assumptions are documented in Table 3 in the appendix. The assumptions are closely based on the technical descriptions and measurement data of the facilities documented in the literature (Jensen & PlanEnergi, 2014; Sifnaios et al., 2022; Sørensen & Schmidt, 2018). Combining geometry data, a reference system, and standardized processes (ecoinvent database) provides a realistic and reproducible basis for balancing material and energy flows.

To reduce complexity, the PTES has been divided into five functional modules: Earthworks; Ground Liner; Cover System; and System Components (Inlet/Outlet; Pumps; and Water Content). This division makes analysis easier and enables contributions within the system to be clearly allocated. We have modeled two variants of the cover system, which differ only in terms of ballasting. Variant A corresponds to the original design with HDPE weight pipes filled with concrete. Variant B is the revised version with a layer of gravel as ballast. Both variants were accounted for separately and included in the LCI. Table 1 provides an overview of the modules and materials.

Table 1: Main LCI components of the reference PTES system.
The central modules, the most important materials, and their respective functions are shown (process and quantity data are listed in Table 3 in the appendix).

Module	Main component / material	Key assumption	Function / description
Earthworks	Excavation (soil)	Excavated volume ≈ 80 000 m³	Creation of the pit and embankment using local soil.
Ground liner	HDPE geomembrane + PP geotextile	Total area ≈ 12 000 m²	Sealing of bottom and side walls; geotextile as mechanical protection.
Cover system	Floating cover with PE foam insulation	Three layers, total 240 mm	Thermal insulation and water protection; main impact driver of PTES.
Cover variant A	Concrete-filled HDPE weight pipes	~50 t concrete ballast	Stabilization and rainwater drainage (original SUNSTORE 4 design).
Cover variant B	Gravel ballast layer	~50 t gravel	Replacement of weight pipes; improved constructability and lower GWP.
Inlet / outlet	Stainless steel pipes	~6 t steel	Stratified charge/discharge of storage water.
Pumps	Centrifugal pumps	8 units	Circulation and rainwater removal.
Water content	Treated (deionized) water	~77 000 m³	Thermal storage medium.

4.2. Life Cycle Impact Assessment (LCIA)

In this chapter, we present the results of the impact assessment for the modeled reference system. The focus is on global warming potential (GWP_{100}), which is expressed in kg CO_2-eq. Additional impact categories are listed in Table 4 in the appendix for the two coverage variants.

The LCIA shows that the two deck variants differ only slightly. Variant A is around 539 t CO_2 eq, variant B around 525 t CO_2 eq; the difference of around 3% is within the assumed ±20% uncertainty range. The concrete (approx. 50 t) in variant A has an impact of approx. 6.7 t CO_2 equivalent and a share of 1.25%, and is therefore not a dominant factor; from this point on, we consider both variants to be equivalent and use variant B for further calculations. The largest shares are accounted for by the covering materials: PE foam (44.6%, ≈ 233 t CO_2 eq), HDPE cover liner (16.3%, ≈ 85 t CO_2 eq) and ground liner (HDPE + geotextile) (14.5%, ≈ 76 t CO_2 eq). Earthworks also exceed the 5 % threshold at 9 %, as does the steel inlet/outlet system at 7.5 %. Smaller contributions are shown in Table 5 in the appendix. Together, these confirm the impact driver is the cover for the cradle-to-gate balance: PE foam and HDPE cover liner together accounting for around 61 %; see Figure 2 for relative shares (left) and absolute contributions (right).

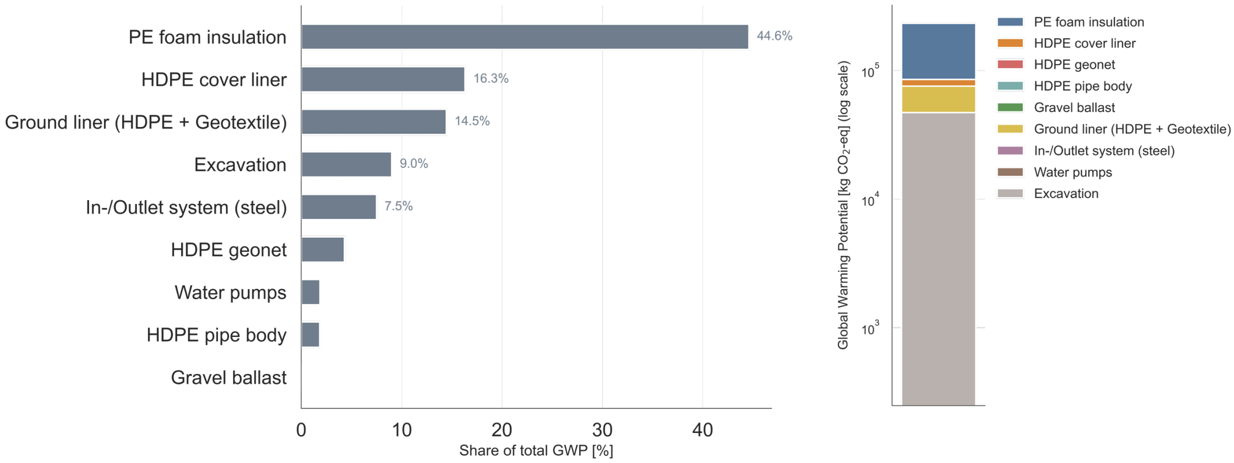

Figure 2: Figure 2: Life cycle impact and component contributions of the reference PTES. The left panel shows the relative share of each component in the total GWP_{100} [%]. The right panel shows the absolute contribution of each component [kg CO_2-eq]; the total is ≈5.24×10^5 kg CO_2-eq (cradle-to-gate, variation A cover design).

Specific GWPs can also be derived from the absolute results. The calculation refers to the FU, i.e., the annual amount of heat stored by the reference system. One charging cycle per year was assumed for modeling. With a storage volume of 76,929 m³ and a storage capacity of 6.96 GWh (≈90 kWh/m³ energy density). This results in a specific GWP of around a specific GWP of around 76 kg CO_2 eq/MWh and 6.9 kg CO_2 eq/m³.

4.3. Scaling Analysis

This section quantifies the relationship between storage volume and climate impact. The analysis is carried out within a cradle-to-gate framework based on annual FU with one charging cycle per year and constant energy density. We assume form invariance, i.e., the slope angle, aspect ratio, and layer thickness remain the same across all sizes. The balance is dominated by the cover materials made of PE foam and HDPE film, but this alone does not reach the dominance threshold of at least 70–80% for Case 1. We therefore use Case 2, an additive multi-term model with area-related proportions $\propto V^{2/3}$ and volumetric proportions $\propto V$.

In our scaling model, implemented in Python, we consider three terms with pronounced volume dependence: the cover area (61%), the liner area of the bottom and sides (14.5%), and the excavation (9%). Together, these proportions cover around 84 – 85% of the total GWP and thus determine the scaling. All other contributions show no reliable dependence on volume in the size range under consideration and are treated as a constant residual. The term intensities αi are derived from the reference case by dividing the respective LCIA impact of a component group by the corresponding geometric variable, for example $\alpha_{\mathrm{cove}} = \frac{\mathrm{GWP(PE\ foam + HDPE\ cover\ liner)}}{A_{\mathrm{cover}}}$. We specify the margin of error as ±20%. The relevant areas and volumes are calculated from the reference geometry for a series of volumes. $GWP_{tot}(V)$ is then determined and normalised to $GWP_{spec}(V)$ [kg CO_2-eq/MWh]. A power function, a V^b, is fitted to the resulting point pairs (V, GWP_{spec}). For the run shown in Figure 3, this results in a ≈ 1793.1 and b ≈ −0.281.

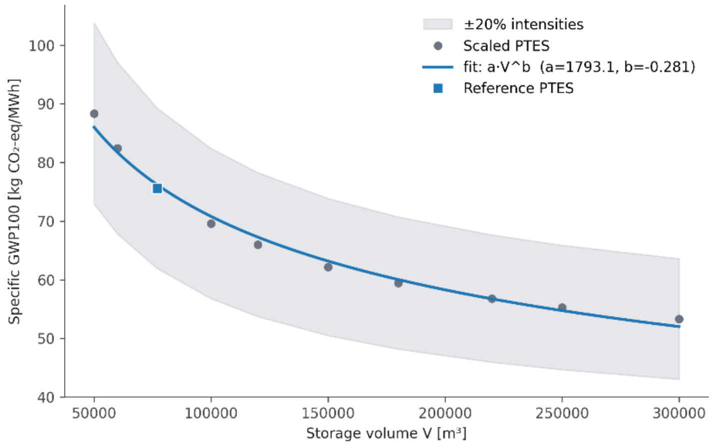

Figure 3: Specific GWP_{100} in kg CO_2-eq/MWh as a function of storage volume V for PTES (variant B). Points: Results of the Case 2 model from the Python tool based on the reference geometry and LCIA intensities. Line: Power fit; gray band: ±20% intensity uncertainty; blue square: reference storage, cradle-to-gate and defined FU.

4.4. Limitations

Like any LCA, this study has limitations: (i) It applies a cradle-to-gate system boundary rather than a full life-cycle assessment; operation, maintenance, and end-of-life are excluded, so potential trade-offs with operational losses or efficiency gains are not captured and must be added for holistic decisions. (ii) Results are strongly shaped by the FU and reference assumptions, particularly the energy density, one cycle per year, and a 25-year lifetime; deviations shift GWP_{spec}, so project-specific sensitivities should be reported. (iii) Scaling relies on form invariance; very small PTES with high fixed shares and very large storages with additional structural requirements may violate this assumption and therefore require parameter recalibration or additional terms. (iv) Background data and α-values are simplified, modeled with ecoinvent 3.9.1 and a ±20% range; location- and supply-chain-specific differences and alternative manufacturing routes can cause larger variation and should be reflected where possible. (v) Transferability and model reduction are limited. The approach is calibrated to the SUNSTORE 4 reference; simplify relationships and may obscure interactions, hence for different designs or materials the impact driver should be re-identified, parameters adjusted, and results not carried over to other impact categories without further analysis. (vi) In the LCI we use simplified proxy processes to represent materials where real manufacturing routes and supplier-specific data were unavailable; this increases consistency but can under- or over-estimate component-level contributions. Where project data are accessible, proxies should be replaced and results updated. (VIII) Unscaled residual contributions: Approximately 15 % of the effect is modeled as a constant residual. For small or very large volumes, their relative significance may increase.

4.5. Outlook

The next step is to validate the scaling functions. To do this, we are testing the Case 2 approach on real plants with different volumes and geometries and calibrating the parameters in the event of deviations. At the same time, we will gradually replace proxy processes in the LCI with project- and manufacturer-specific data (material compositions and densities, location-specific transport, real manufacturing routes, recycling rates). To account for uncertainty, we recommend an extended analysis that goes beyond ±20%. It should include scenarios for energy density, cycle count, and service life, correlations between α values, and Monte Carlo simulations for background and transport data. The results should be reported as ranges with sensitivities. Methodologically, we examine the limits of form invariance (very small storage facilities with fixed proportions, very large storage facilities with additional structural measures) and the role of residual contributions that are not currently scaled. Finally, the approach can be transferred to other STES types (e.g., TTES) and expanded to include operating and end-of-life phases and additional impact categories.

5. Conclusion

This study shows how the GWP of PTES can be estimated in early planning phases. To do this, we identify the impact driver and scale it using fixed geometric properties. The LCIA carried out proves that the use of PE foam and HDPE films is decisive for the ecological coverage of PTES. Design details of the ballast do not significantly influence the GWP within the scope of the study. An additive multi-term model is used for scaling: area proportions scale with $V^{2/3}$, volume proportions with V, and a small remainder is kept constant. This allows specific emissions to be estimated based on size without having to set up a complete LCA for each storage size. Secondly, the scaling shows clearly sublinear behavior. As the volume increases, the specific GWP decreases, while the absolute emissions increase. In practice, this means that although larger storage facilities are more climate-friendly per MWh stored, their construction is not emission-free. Results should always be reported as ranges. We vary the intensities of the terms by ±20%, which defines the uncertainty band shown in Figure 3. From a planning perspective, this results in the following simple order of priority: (1) Optimize cover material paths and layer thicknesses (PE foam, HDPE films), (2) Select size, this is where the sublinear economies of scale come into play, (3) Subordinate ballasting, as its influence on the GWP is low. The parameters reported here refer to cradle-to-gate, an annual FU (one cycle per year), and the form invariance of the geometry. The scope of these conclusions is cradle-to-gate and assumes form invariance and the specified reference assumptions. Looking ahead, validation at other plants and the replacement of proxy processes with real manufacturing and supply chain data are obvious next steps, as is the expansion to include operation and end-of-life. This will allow the approach to be further refined and transferred to other STES types such as tank thermal energy storage, provided that the respective impact driver is clearly identified.

6. Acknowledgments

This dissertation resulted from research within the research project "Sociotechnological Breakthrough of Thermal Energy Storage - a new Approach of Constructive Technology Assessment" (contract No. CRSII5_202239), financed by the Swiss National Science Foundation. The author would like to thank the Swiss National Science Foundation for their financial support.

During the preparation of this work, the author used Grammarly and DeepL for linguistic editing and revision, and ChatGPT for editorial feedback. After using these tools, the author reviewed and edited the content as needed and takes full responsibility for the dissertation's content.

7. References

Alva, G., Lin, Y., & Fang, G. (2018). An overview of thermal energy storage systems. *Energy*, *144*, 341–378. https://doi.org/10.1016/j.energy.2017.12.037

Arvidsson, R., Tillman, A. M., Sandén, B. A., Janssen, M., Nordelöf, A., Kushnir, D., & Molander, S. (2018). Environmental Assessment of Emerging Technologies: Recommendations for Prospective LCA. *Journal of Industrial Ecology*, *22*(6), 1286–1294. https://doi.org/10.1111/JIEC.12690

Bott, C., Dressel, I., & Bayer, P. (2019). State-of-technology review of water-based closed seasonal thermal energy storage systems. In *Renewable and Sustainable Energy Reviews* (Vol. 113). Elsevier Ltd. https://doi.org/10.1016/j.rser.2019.06.048

de Gracia, A., & Cabeza, L. F. (2015). Phase change materials and thermal energy storage for buildings. *Energy and Buildings*, *103*, 414–419. https://doi.org/10.1016/j.enbuild.2015.06.007

Gaegauf, C., Sattler, M., Dorer, V., Orehounig, K., Zweifel, G., Bless, C., Bergmann, T., & Del Duce, A. (2016). SPEQUA – Thermische und elektrische Spei-cher in Gebäuden und Quartieren. *Bundesamt Für Energie*.

Godinaud, J., Loubet, P., Gombert-Courvoisier, S., Pryet, A., Dupuy, A., & Larroque, F. (2024). Life Cycle Assessment of an Aquifer Thermal Energy Storage System: Influence of design parameters and comparison with conventional systems. *Geothermics*, *120*(March), 102996. https://doi.org/10.1016/j.geothermics.2024.102996

Hayatina, I., Auckaili, A., & Farid, M. (2023). Review on the Life Cycle Assessment of Thermal Energy Storage Used in Building Applications. *Energies*, *16*(3), 1170. https://doi.org/10.3390/en16031170

Jensen, M. V., & PlanEnergi. (2014). *IEA-SHC TECH SHEET, Task 45 Large Systems Description: Guidelines for design of seasonal pit heat storages*. http://task45.iea-shc.org/fact-sheets

Lüchinger, R., Hendry, R., Walter, H., Worlitschek, J., & Schuetz, P. (2025). Cost Analysis for Large Thermal Energy Storage Systems. *ASME. J. Eng. Sustain. Bldgs. Cities*, *JESBC-25-1*(6(2): 021006), 14. https://doi.org/https://doi.org/10.1115/1.4069122

Ni, Z., Wang, Y., Wang, Y., Chen, S., Xie, M., Grotenhuis, T., & Qiu, R. (2020). Comparative Life-Cycle Assessment of Aquifer Thermal Energy Storage Integrated with in Situ Bioremediation of Chlorinated Volatile Organic Compounds. *Environmental Science and Technology*, *54*(5), 3039–3049. https://doi.org/10.1021/ACS.EST.9B07020/ASSET/IMAGES/LARGE/ES9B07020_0002.JPEG

Pallotta, G., Marrasso, E., Martone, C., Luciano, N., Squarzoni, G., Roselli, C., & Sasso, M. (2025). Aquifer thermal energy storage for decarbonising heating and cooling energy supply in southern Europe: A dynamic environmental impact assessment. *Applied Energy*, *394*, 126105. https://doi.org/10.1016/J.APENERGY.2025.126105

Shah, S. K., Aye, L., & Rismanchi, B. (2018). Seasonal thermal energy storage system for cold climate zones: A review of recent developments. *Renewable and Sustainable Energy Reviews*, *97*, 38–49. https://doi.org/10.1016/j.rser.2018.08.025

Sifnaios, I. (2023). *Investigations of pit thermal energy storages in district heating systems*. https://doi.org/10.11581/DTU.00000291

Sifnaios, I., Sifnaios, I., Jensen, A., Furbo, S., & Fan, J. (2022). Effect of Design Characteristics on Pit Thermal Energy Storage (PTES) Performance. *Proceedings of EuroSun 2022 - ISES and IEA SHC International Conference on Solar Energy for Buildings and Industry*, 1–7. https://doi.org/10.18086/eurosun.2022.13.21

Sørensen, A., & Schmidt, T. (2018). Design and Construction of Large Scale Heat Storages for District Heating in Denmark. *International Conference on Energy Storage*, *April*. http://planenergi.dk/wp-content/uploads/2018/05/Soerensen-and-Schmidt_Design-and-Construction-of-Large-Scale-Heat-Storages-12.03.2018-004.pdf

Sorknæs, P. (2018). Simulation method for a pit seasonal thermal energy storage system with a heat pump in a district heating system. *Energy*, *152*, 533–538. https://doi.org/10.1016/J.ENERGY.2018.03.152

Sträter, R., Lüchinger, R., & Zumofen, G. (2025). Exploring the market and community acceptance of seasonal thermal energy storage technologies: Insights from a population survey in Switzerland. *Energy Research & Social Science*, *121*, 103954. https://doi.org/10.1016/J.ERSS.2025.103954

Venettacci, S., Cozzolino, R., Ponticelli, G. S., & Guarino, S. (2022). Environmental and economic life cycle assessment of thermal energy storage based on organic phase change material embedded in open-cell copper foams. *Sustainable Production and Consumption*, *29*, 387–405. https://doi.org/10.1016/J.SPC.2021.10.026

Welsch, B., Göllner-Völker, L., Schulte, D. O., Bär, K., Sass, I., & Schebek, L. (2018). Environmental and economic assessment of borehole thermal energy storage in district heating systems. *Applied Energy*, *216*, 73–90. https://doi.org/10.1016/J.APENERGY.2018.02.011

Welsch, B., Rühaak, W., Schulte, D. O., Bär, K., & Sass, I. (2016). Characteristics of medium deep borehole thermal energy storage. *International Journal of Energy Research*, *40*(13), 1855–1868. https://doi.org/10.1002/ER.3570

Wu, X., Sameti, M., Nasiri, F., & Li, B. (2024). An off-grid solar district energy system with borehole thermal energy storage: Life cycle assessment in a subarctic region. *Journal of Building Engineering*, *91*, 109576. https://doi.org/10.1016/j.jobe.2024.109576

Xiang, Y., Xie, Z., Furbo, S., Wang, D., Gao, M., & Fan, J. (2022). A comprehensive review on pit thermal energy storage: Technical elements, numerical approaches and recent applications. *Journal of Energy Storage*, *55*, 105716. https://doi.org/10.1016/J.EST.2022.105716

Xu, J., Wang, R. Z., & Li, Y. (2014). A review of available technologies for seasonal thermal energy storage. *Solar Energy*, *103*, 610–638. https://doi.org/10.1016/j.solener.2013.06.006

Yang, T., Liu, W., Kramer, G. J., & Sun, Q. (2021). Seasonal thermal energy storage: A techno-economic literature review. In *Renewable and Sustainable Energy Reviews* (Vol. 139). Elsevier Ltd. https://doi.org/10.1016/j.rser.2021.110732

Zhang, L., Xu, P., Mao, J., Tang, X., Li, Z., & Shi, J. (2015). *A low cost seasonal solar soil heat storage system for greenhouse heating: Design and pilot study*. https://doi.org/10.1016/j.apenergy.2015.07.036

Appendix

Table 2: Main geometric parameters of the reference storage facility (PTES SUNSTORE 4, Marstal). The values are based on Sifnaios et al., (2022) **and serve as the basis for modeling the reference system.**

Parameter	Unit	Value
Side slope	°	25.8
Lid aspect ratio	-	1.28
Bottom side length (a)	m	47.6
Bottom side width (b)	m	22.6
Top side length (A)	m	113.1
Top side width (B)	m	88.1
Sides and bottom area	m²	11 022
Lid area	m²	9 972
Storage height	m	16
Storage volume	m³	76 929

Table 3: LCI inputs assumptions for the reference PTES system.
The table summarizes the main life cycle inventory inputs, material specifications, and modelling assumptions used to represent the reference PTES with two alternative cover designs A and B.

Module	Item	Unit	Quantity*	ecoinvent process	Derivation / assumptions
Earthworks	Excavation of PTES volume and earthworks	m³	80 000	excavation, hydraulic digger; RER	Excavation equals storage volume (76 929 m³) plus allowance for additional work (rounded up).
Ground liner	Geomembrane (HDPE, 2.0 mm)	kg	22 850	polyethylene, high density, granulate; at plant; RER + extrusion, plastic film; RER	Bottom and side liner ≈ 11 000 m² + edge strip ≈ 1 000 m²; t = 2.0 mm; ρ = 950 kg/m³.
Ground liner	Geotextile underliner (PP 500 g/m²)	kg	6 000	geotextile production, polypropylene; RER	A ≈ 12 000 m² × 0.5 kg/m²; protective layer beneath HDPE liner.
Cover	Top liner (1.5 mm)	kg	15 050	polyethylene, high density, granulate; at plant; RER + extrusion, plastic film; RER	Surface area ≈ 10 550 m² incl. 1.5 m edge overlap; ρ = 950 kg/m³.
Cover	Floating bottom liner (2.0 mm)	kg	21 250	polyethylene, high density, granulate; at plant; RER + extrusion, plastic film; RER	Floating layer ≈ 11 200 m² incl. 3 m overlap; ρ = 950 kg/m³.
Cover	Thermal insulation (3 × 80 mm PE foam)	kg	73 250	polyethylene, high density, granulate; at plant; RER + polymer foaming; RER	Three-layer PE foam (Nomalen 28 N); total thickness 240 mm; area ≈ 10 150 m²; ρ = 30 kg/m³.
Cover (A)	Weight pipes – concrete fill	kg	50 000	concrete, normal; at plant; RER	Variant A: with concrete-filled HDPE pipes; ρ = 2 400 kg/m³; geometry based on SUNSTORE-4
Cover (A)	Weight pipes – HDPE pipe body	kg	8 200	polyethylene, high density, granulate; at plant; RER + extrusion, plastic pipes; RER	Variant A: Pipe lengths Ø110 = 672 m, Ø125 = 748 m, Ø140 = 202 m, Ø200 = 56 m; ρ = 950 kg/m³.
Cover (B)	Gravel ballast layer	kg	50 000	gravel, crushed; at mine; RER	Variant B: with gravel ballast replacing concrete weight pipes; assumed 100 mm layer (ρ ≈ 1 800 kg/m³; A ≈ 10 000 m²).
System	Inlet / outlet system	kg	6 000	steel, stainless 18/8; at plant; RER	3 × 100 m; DN 225 mm; t = 5.5 mm; ρ = 8 000 kg/m³; includes three diffusers.
System	Treated water (fill volume)	m³	76 950	water, deionised; at plant; RER	Equal to PTES storage volume
System	Water pumps (for circulation and rainwater removal)	item	8	water pump, 22kW; GLO	Centrifugal pumps and rainwater drainage, plus redundancy

**Table 4: Comparison of ReCiPe 2016 (H) midpoint impact results for the two PTES cover.
The table shows the total impact results per storage system for variant A (concrete-filled weight pipes) and variant B (gravel ballast). The relative reduction [%] indicates the decrease in environmental impacts achieved by substituting concrete with gravel.**

Name	Einheit	Variants A	Variants B	Reduction
acidification: terrestrial no LT - terrestrial acidification potential (TAP) no LT	kg SO2-Eq	1686	1651	-2%
climate change no LT - global warming potential (GWP100) no LT	kg CO2-Eq	538833	523665	-3%
ecotoxicity: freshwater no LT - freshwater ecotoxicity potential (FETP) no LT	kg 1,4-DCB-Eq	593	582	-2%
ecotoxicity: marine no LT - marine ecotoxicity potential (METP) no LT	kg 1,4-DCB-Eq	2034	2001	-2%
ecotoxicity: terrestrial no LT - terrestrial ecotoxicity potential (TETP) no LT	kg 1,4-DCB-Eq	2707662	2671333	-1%
energy resources: non-renewable, fossil no LT - fossil fuel potential (FFP) no LT	kg oil-Eq	302702	295347	-2%
eutrophication: freshwater no LT - freshwater eutrophication potential (FEP) no LT	kg P-Eq	15	15	-2%
eutrophication: marine no LT - marine eutrophication potential (MEP) no LT	kg N-Eq	6	6	-2%
human toxicity: carcinogenic no LT - human toxicity potential (HTPc) no LT	kg 1,4-DCB-Eq	24807	24675	-1%
human toxicity: non-carcinogenic no LT - human toxicity potential (HTPnc) no LT	kg 1,4-DCB-Eq	142033	140083	-1%
ionising radiation no LT - ionising radiation potential (IRP) no LT	kBq Co-60-Eq	2540	2476	-3%
land use no LT - agricultural land occupation (LOP) no LT	m2*a crop-Eq	10692	10327	-3%
material resources: metals/minerals no LT - surplus ore potential (SOP) no LT	kg Cu-Eq	7691	7568	-2%
ozone depletion no LT - ozone depletion potential (ODPinfinite) no LT	kg CFC-11-Eq	0	0	
particulate matter formation no LT - particulate matter formation potential (PMFP) no LT	kg PM2.5-Eq	779	765	-2%
photochemical oxidant formation: human health no LT - photochemical oxidant formation potential: humans (HOFP) no LT	kg NOx-Eq	1688	1655	-2%
photochemical oxidant formation: terrestrial ecosystems no LT - photochemical oxidant formation potential: ecosystems (EOFP) no LT	kg NOx-Eq	1870	1835	-2%
water use no LT - water consumption potential (WCP) no LT	m3	5358	5244	-2%

**Table 5: Breakdown of the total GWP_{100} results by component for both cover variants.
The table lists the contribution of each component to the total climate change impact of the reference PTES.**

Variant	Component	Share [%]	Total GWP_{100} [kg CO_2-eq]
A	PE foam insulation	43.33	233 497
	HDPE cover liner	15.86	85 456
	HDPE geonet	4.19	22 600
	HDPE pipe body	3.43	18 500
	Concrete (weight pipes)	*1.25*	*6 714*
	Ground liner (HDPE + Geotextile)	14.05	75 692
	In-/Outlet system (steel)	7.29	39 307
	Water pumps	1.82	9 803
	Excavation	8.77	47 240
	Total	**100 %**	**538 833**
B	PE foam insulation	44.6	233 497
	HDPE cover liner	16.3	85 456
	HDPE geonet	4.32	22 599
	HDPE pipe body	1.85	9 701
	Gravel ballast	*0.07*	*344*
	Ground liner (HDPE + Geotextile)	14.5	75 692
	In-/Outlet system (steel)	7.51	39 307
	Water pumps	1.87	9 803
	Excavation	9.02	47 240
	Total	**100 %**	**523 639**